Supplementary material

Formation Kinetics and Antimicrobial Activity of Silver Nanoparticle Dispersions Based on N-Reacetylated Oligochitosan Solutions for Biomedical Applications

Ekaterina K. Urodkova [1,*], Ol'ga Ya. Uryupina [1], Vladimir E. Tikhonov [2], Natalia E. Grammatikova [3], Anastasia V. Bol'shakova [1], Anna A. Sinelshchikova [1], Alexandra I. Zvyagina [1], Dmitry N. Khmelenin [4], Elena S. Zhavoronok [5] and Ivan N. Senchikhin [1,*]

[1] A.N. Frumkin Institute of Physical Chemistry and Electrochemistry, Russian Academy of Sciences, 119071 Moscow, Russia; urupina635@mail.ru (O.Y.U.)

[2] A.N. Nesmeyanov Institute of Organoelement Compounds, Russian Academy of Sciences, 119991 Moscow, Russia; tikhon@ineos.ac.ru

[3] G.F. Gause Institute of New Antibiotics, 119021 Moscow, Russia; ngrammatikova@yandex.ru

[4] A.V. Shubnikov Institute of Crystallography, Russian Academy of Sciences, 119333 Moscow, Russia

[5] Lomonosov Institute of Fine Chemical Technologies, MIREA—Russian Technological University, 119571 Moscow, Russia

* Correspondence: urodkovakatja@mail.ru (E.K.U.); isenchikhin@gmail.com (I.N.S.)
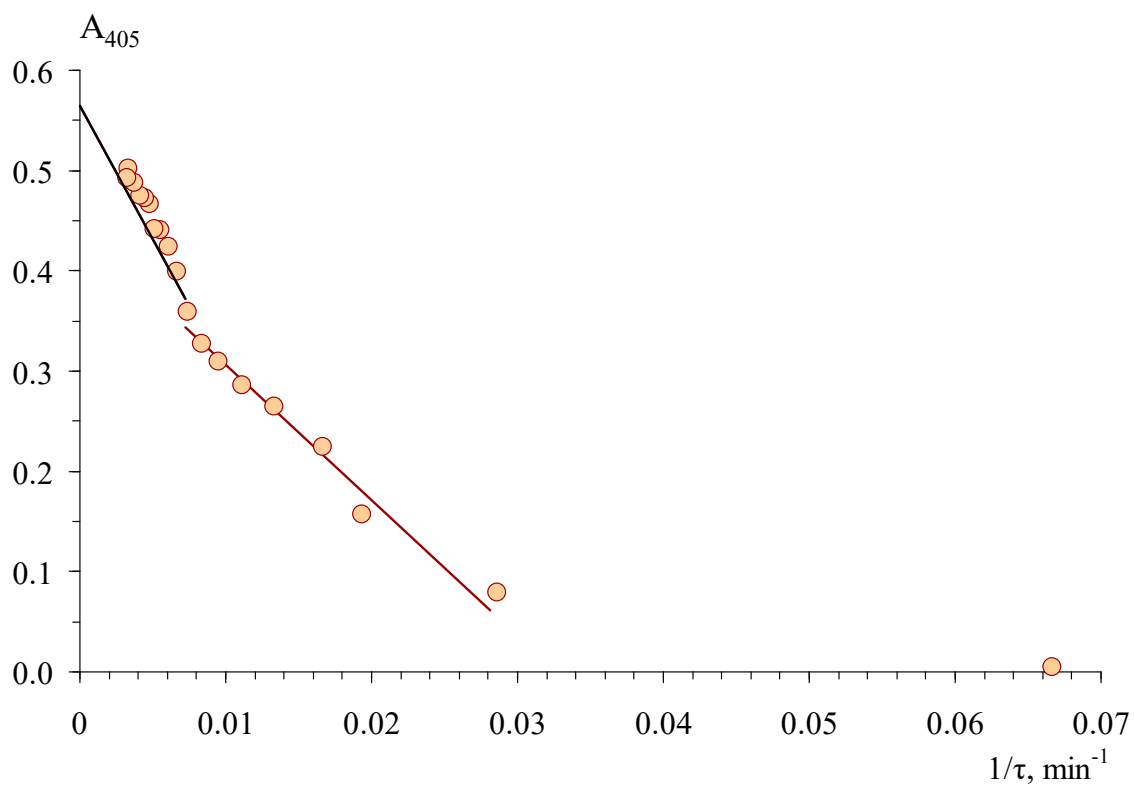
Contents

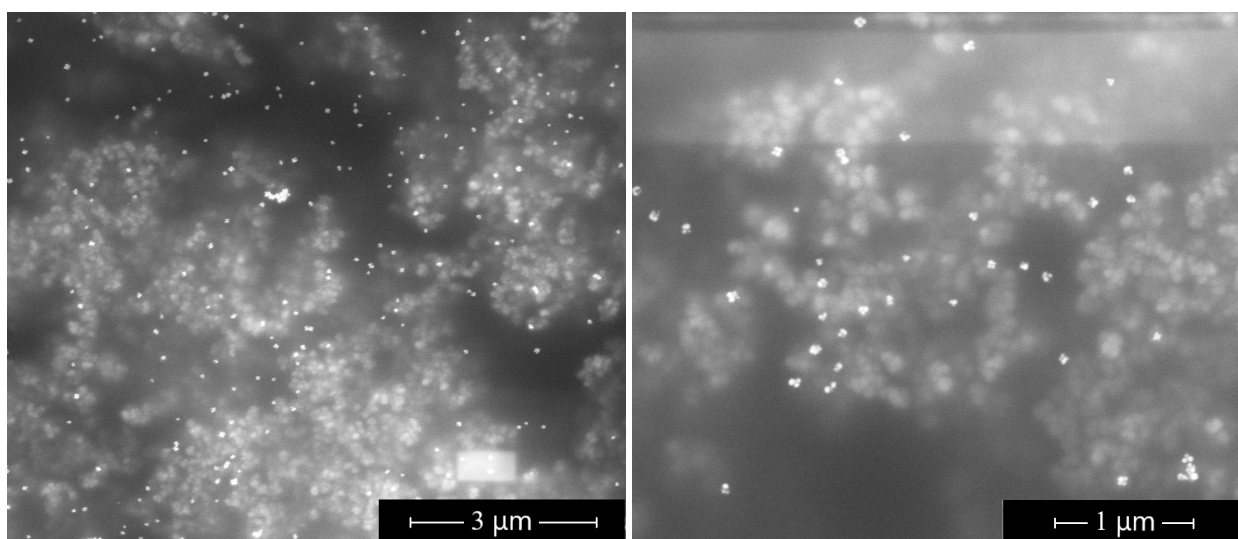Figure S1. Dependence of LSPR peak maximum on inverse time.

Figure S2. SEM images of silver nanoparticles obtained by drying a drop of washed dispersion on a silicon substrate.

Table S1. PXRD qualitative analysis of samples.

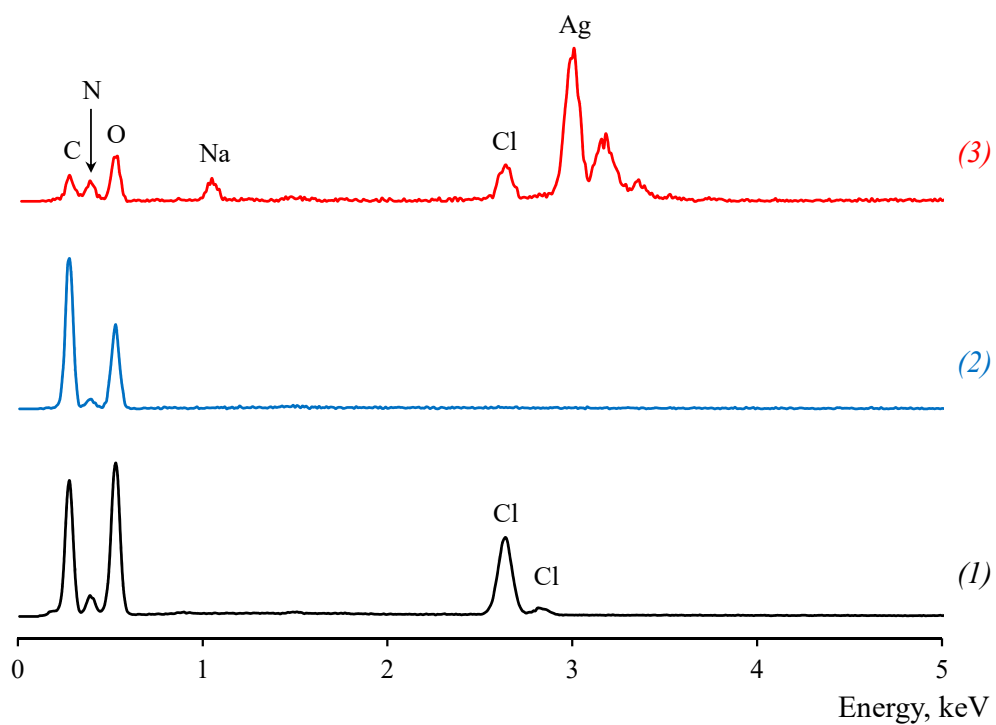| Experiment			The most close phase (PDF2)			
d, Å	Presence of a peak in the experimental diffractogram / I, %		Space group	Cell parameters	d, Å / I, %	hkl
	OChT-12/24-R	OChT-12/25-R*				
Phase I (Fig. 6)			Fm3m	a = 4.085 Å	Ag (4-783)	
2.363	+ / 60	+ / 100			2.332 / 100	111
2.048	+ / 16	+ / 18			2.019 / 45	200
1.446	+ / 15	+ / 20			1.428 / 20	220
1.233	+ / 17	+ / 28			1.218 / 22	311
Phase II (Fig. 6)			Fm3m	a = 5.549 Å	AgCl (31-1238)	
3.210	+ / 46	–			3.200 / 50	111
2.780	+ / 100	–			2.770 / 100	200
1.965	+ / 52	–			1.962 / 60	220
1.675	+ / 13	–			1.670 / 18	311

Figure S3. EDX-spectra of initial OChT-12/24-R (*1*), initial OChT-12/25-R* (*2*) and AgNPs dispersion based on OChT-12/24-R (*3*).
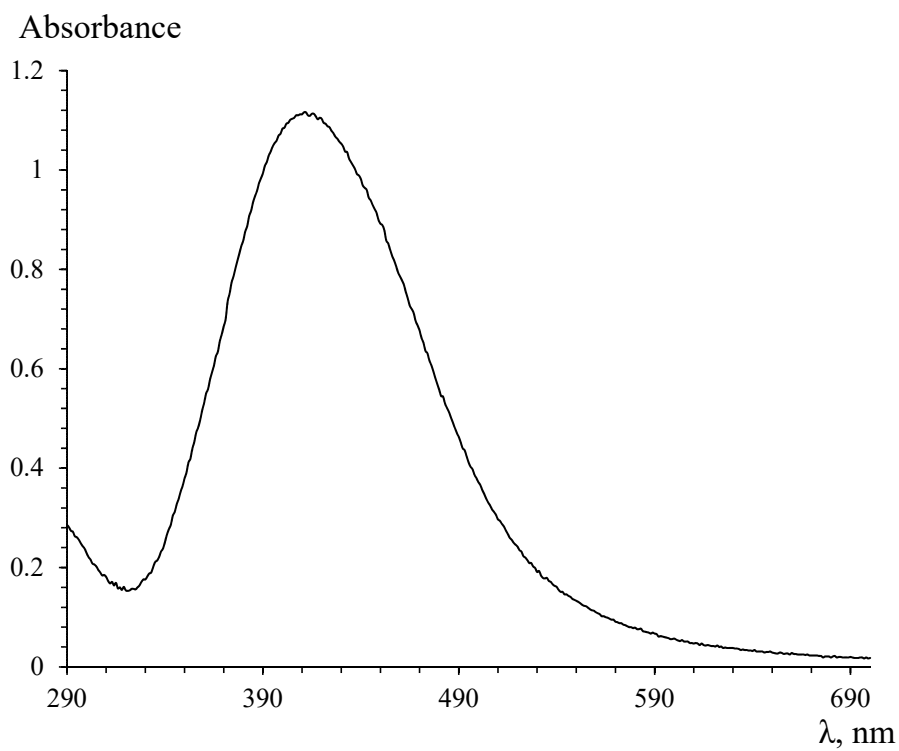

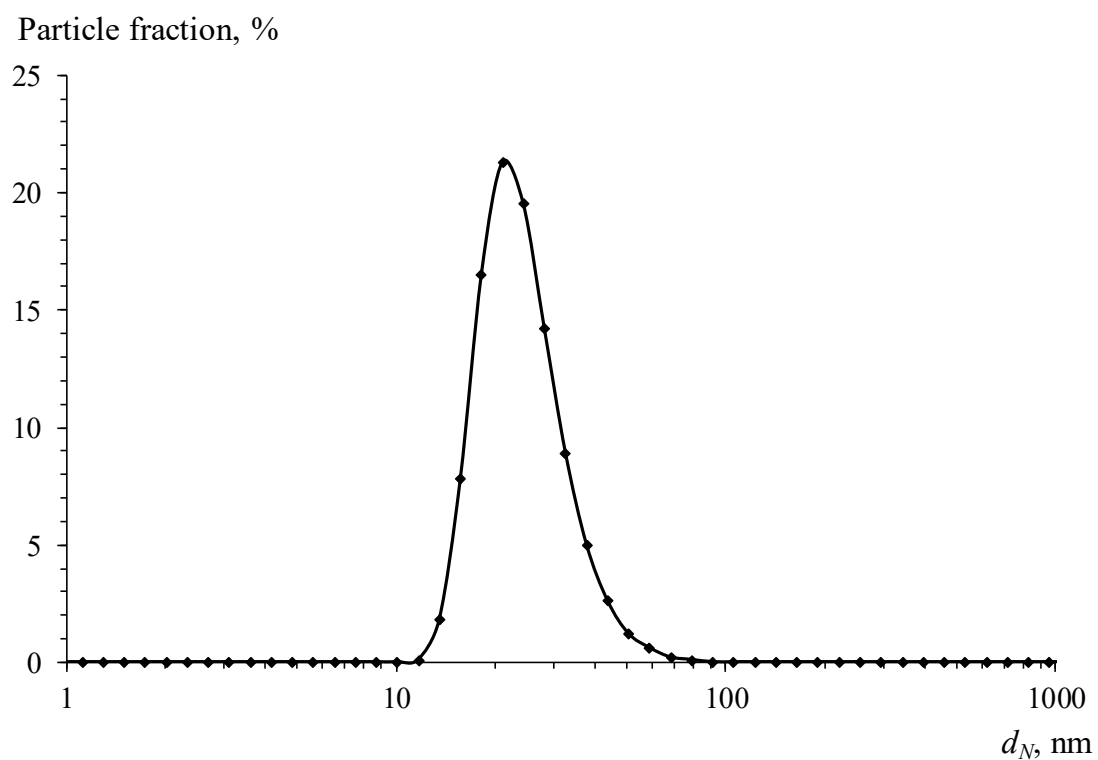Figure S4. Typical UV-visible spectrum of dispersion based on OChT-12/25-R*.

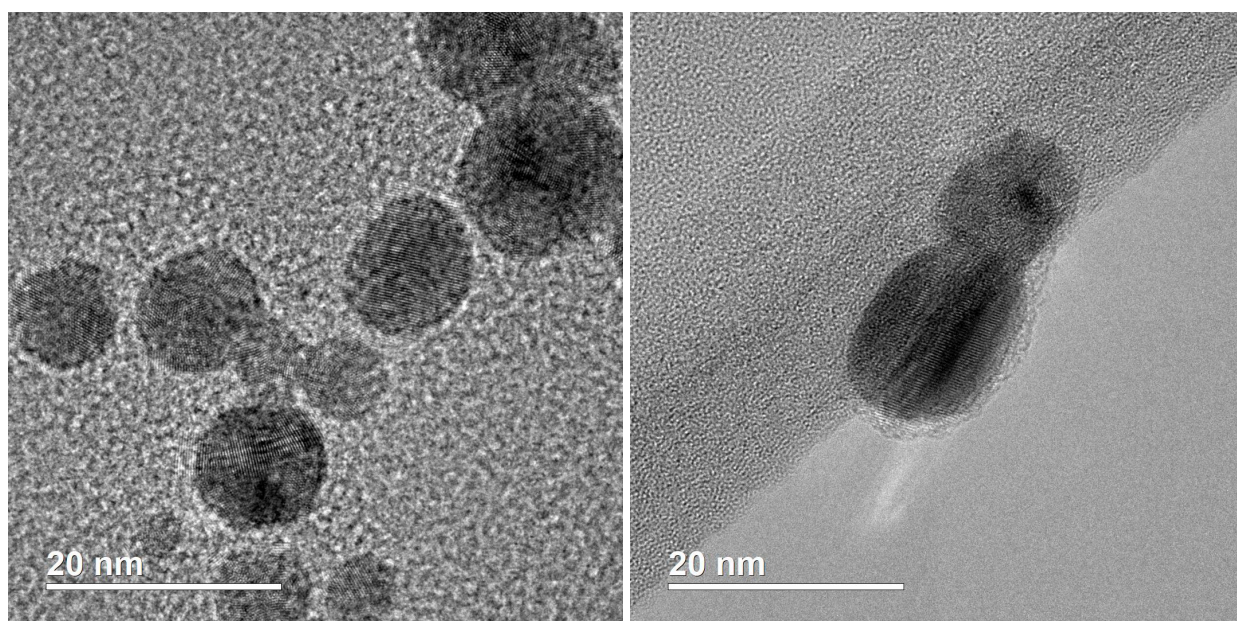Figure S5. Typical particle size distributions of dispersion based on OChT-12/25-R*.

Figure S6. HRTEM images of dispersion stabilized by OChT-12/25-R*.